

Supplementary Materials

Co-Sintering of $\text{Li}_{1.3}\text{Al}_{0.3}\text{Ti}_{1.7}(\text{PO}_4)_3$ and LiFePO_4 in Tape-Casted Composite Cathodes for Oxide Solid-State Batteries

1. Characterization of solid electrolyte and cathode active materials

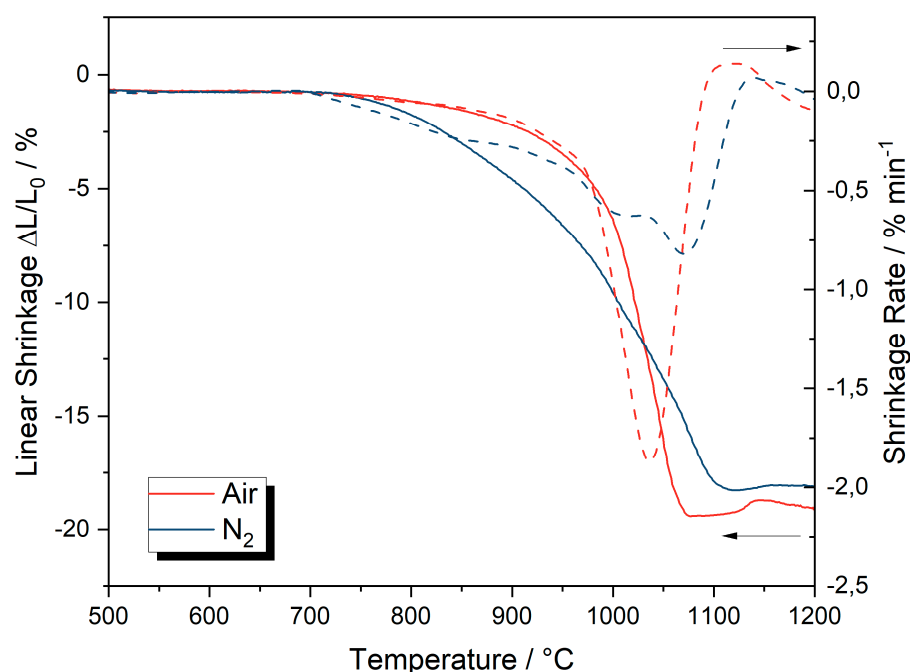


Figure S1. Comparison of the temperature-dependent shrinkage behavior of $\text{Li}_{1.3}\text{Al}_{0.3}\text{Ti}_{1.7}(\text{PO}_4)_3$ in air and N_2 .

The temperature-dependent shrinkage behavior of the LATP solid electrolyte shows an atmospheric dependence. Sintering in air leads to a linear shrinkage of -19.4% in the temperature range 950–1080 °C. The shrinkage curve indicates a single-step process with a shrinkage rate of up to -1.9 %/min at 1035 °C. The shrinkage behavior of LATP in inert atmosphere leads to an extended temperature range of shrinkage from 750 to 1100 °C. A maximum linear shrinkage of -18.3% is achieved. The temperature-dependent shrinkage rate indicates a multi-step shrinkage process during sintering in an inert atmosphere. High shrinkage rates are observed at 840, 1015 and 1070 °C. These correlate with the melting temperatures of $\text{Li}_4\text{P}_2\text{O}_7$ (885 °C) and LiTiOPO_4 (1085 °C) and may therefore indicate liquid-phase sintering.

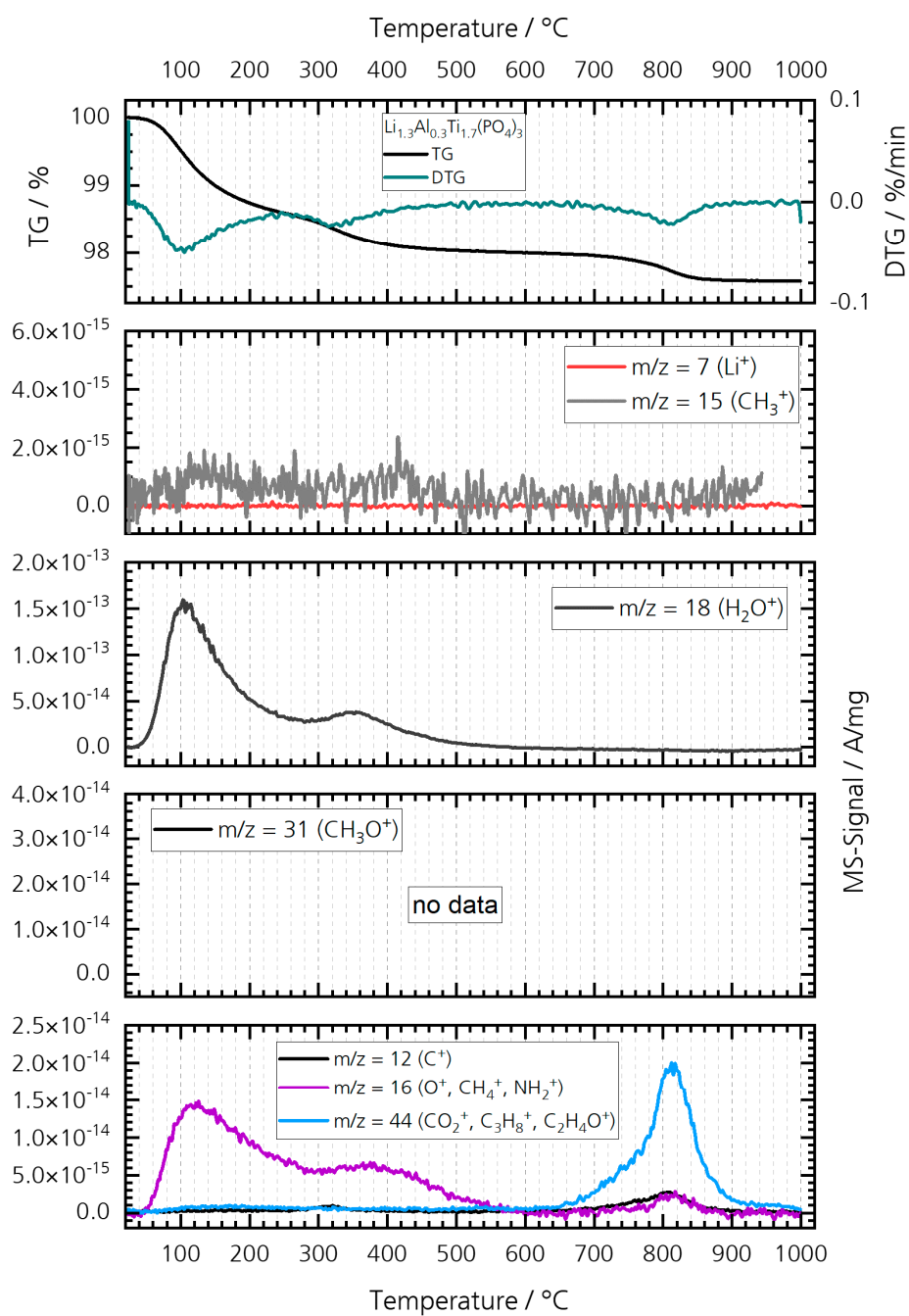


Figure S2. Thermogravimetry (TG) and differential thermogravimetry as first derivation (DTG) of pristine $\text{Li}_{1.3}\text{Al}_{0.3}\text{Ti}_{1.7}(\text{PO}_4)_3$ in N_2 . Selected temperature-dependent m/z data with corresponding possible molecular fragments are shown.

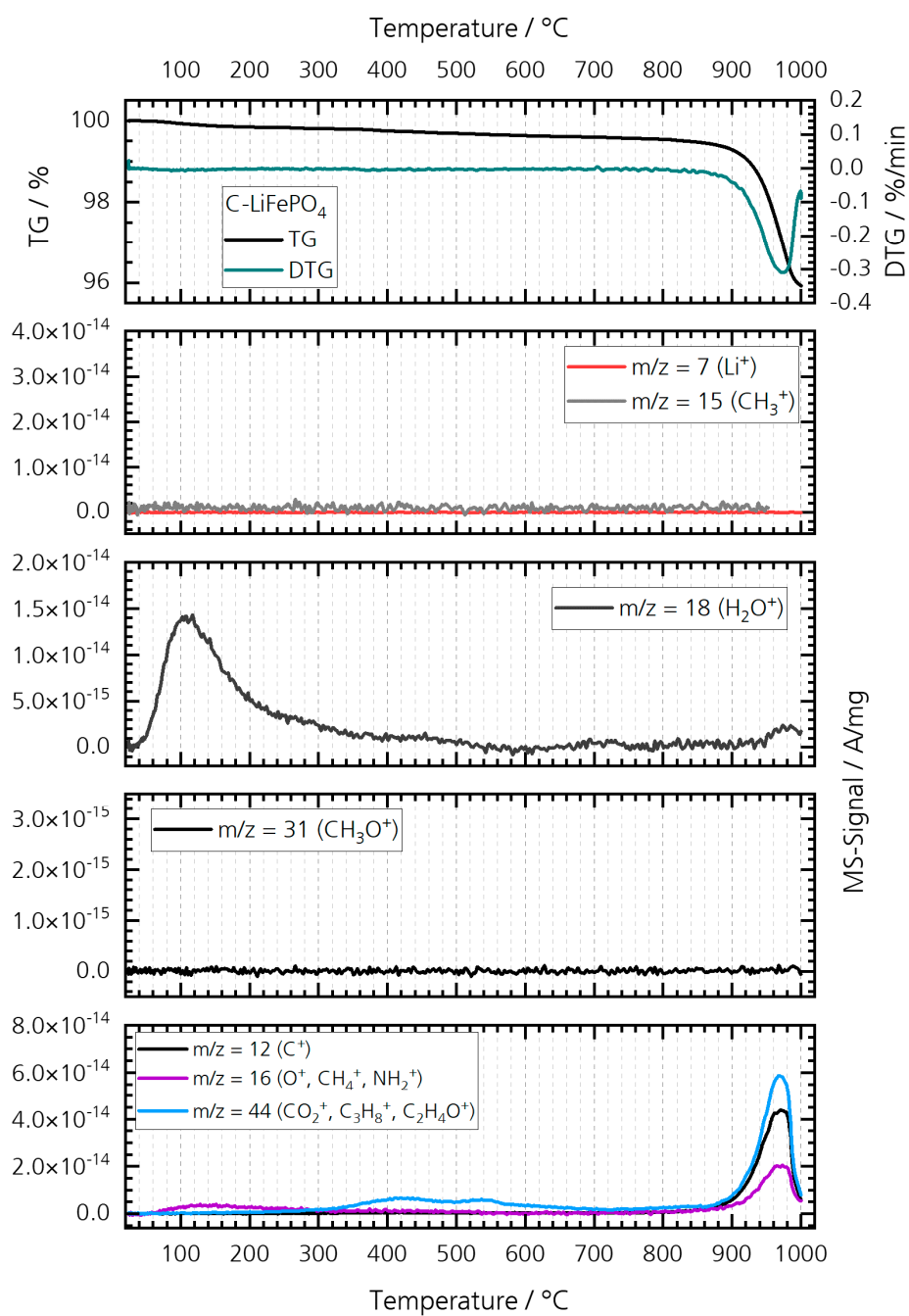


Figure S3. Thermogravimetry (TG) and differential thermogravimetry as first derivation (DTG) of LiFePO_4 in N_2 . Selected temperature-dependent m/z data with corresponding possible molecular fragments are shown.

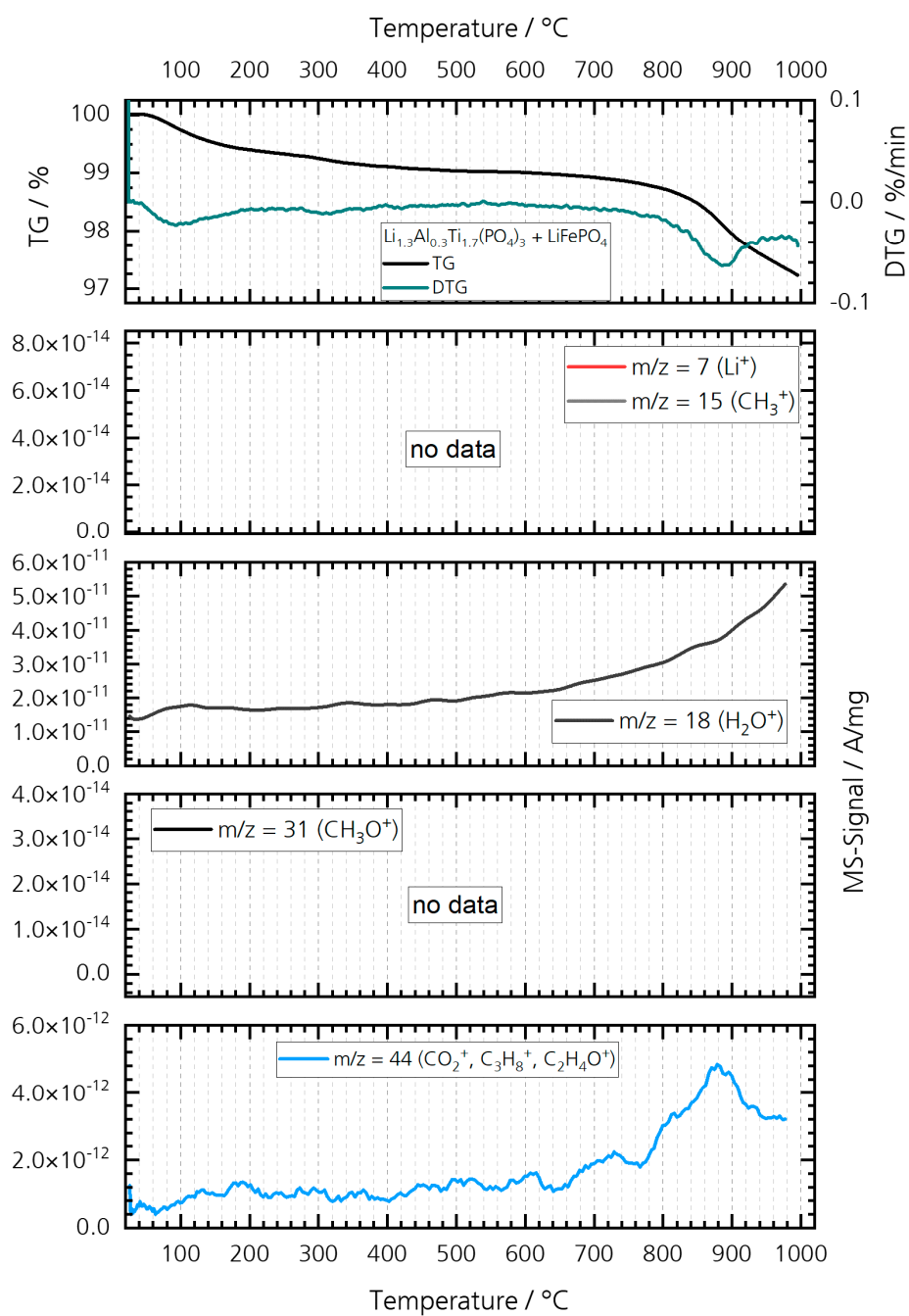


Figure S4. Thermogravimetry (TG) and differential thermogravimetry as first derivation (DTG) of mixture of LiFePO_4 (50 wt%) and $\text{Li}_{1.3}\text{Al}_{0.3}\text{Ti}_{1.7}(\text{PO}_4)_3$ (50 wt%) in N_2 . Selected temperature-dependent m/z data with corresponding possible molecular fragments are shown.

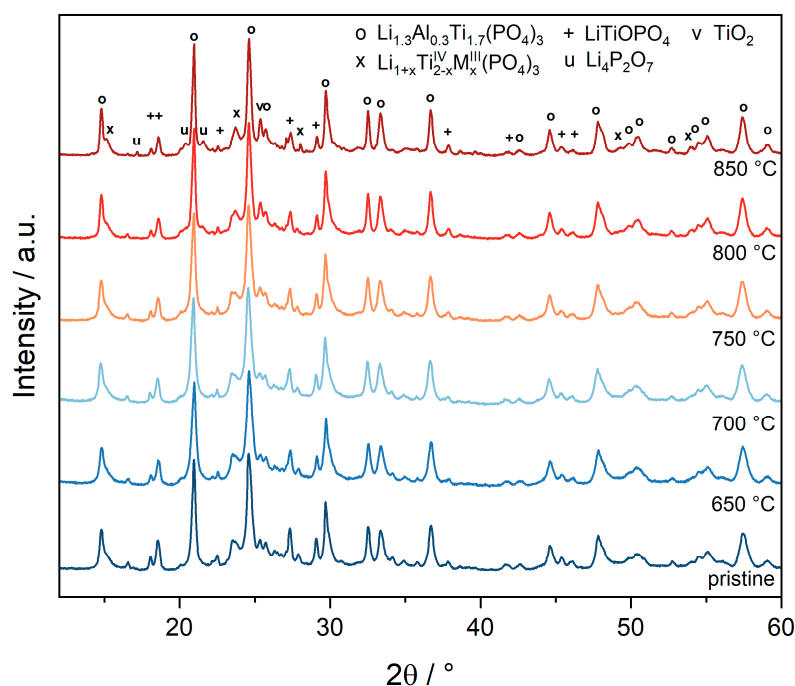


Figure S5. X-Ray diffraction of LATP after heat treatment at N₂ between 650 and 850 °C.

$\text{Li}_{1.3}\text{Al}_{0.3}\text{Ti}_{1.7}(\text{PO}_4)_3$ is identified as the main crystalline phase. Further secondary phases are orthorhombic $\text{Li}_{1+x}\text{M}_x\text{Ti}_{2-x}(\text{PO}_4)_3$ ($\text{M} = \text{Al}^{3+}, \text{Ti}^{3+}; x > 0.5$), LiTiOPO_4 , TiO_2 and $\text{Li}_4\text{P}_2\text{O}_7$. Additional amorphous phases may not be excluded. Heat treatment at inert atmosphere leads to increased formation of an orthorhombic $\text{Li}_{1+x}\text{M}_x\text{Ti}_{2-x}(\text{PO}_4)_3$ ($\text{M} = \text{Al}^{3+}, \text{Ti}^{3+}$) phase. In addition, the formation of $\text{Li}_4\text{P}_2\text{O}_7$ is detected at $T > 800$ °C.

Table S1. Lattice parameters of $\text{Li}_{1.3}\text{Al}_{0.3}\text{Ti}_{1.7}(\text{PO}_4)_3$ after sintering in N₂.

Temperature / °C	a / Å	c / Å	V / Å ³	Primary Particle size / nm
pristine	8.495(5)	20.86(2)	1303.9(2)	61±2
650	8.496(6)	20.87(2)	1304.8(2)	47±1
700	8.497(6)	20.88(2)	1304.8(2)	50±1
750	8.496(5)	20.88(2)	1305.1(2)	57±1
800	8.498(4)	20.87(2)	1305.7(2)	74±2
850	8.498(3)	20.87(1)	1305.2(1)	90±2

The LATP lattice parameters a and c are constant with increasing sintering temperatures, whereas the cell volume increases with higher sintering temperatures. In addition, the crystallite size of the primary particles increases with higher sintering temperatures, indicating crystal growth during heat treatment.

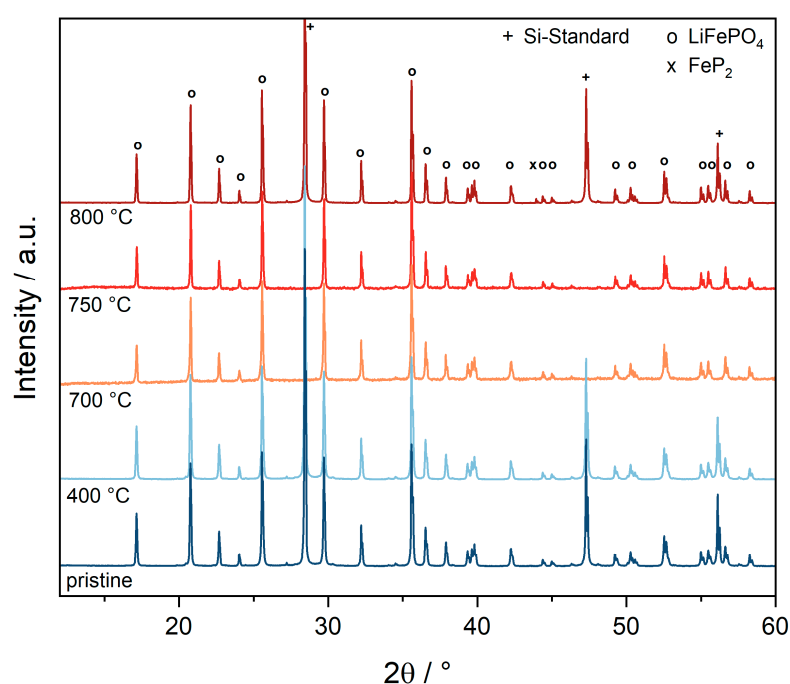


Figure S6. X-ray diffraction of LFP after heat treatment in N_2 between 400 and 800 °C. Si has been added to selected samples as an internal standard. LiFePO_4 does not show any decomposition reactions up to a temperature of 750 °C. The formation of FeP_2 is detectable from a sintering temperature of $T > 800$ °C.

2. FESEM-EDX mappings of co-sintered LATP-LFP pellets and tape-casted composite cathodes

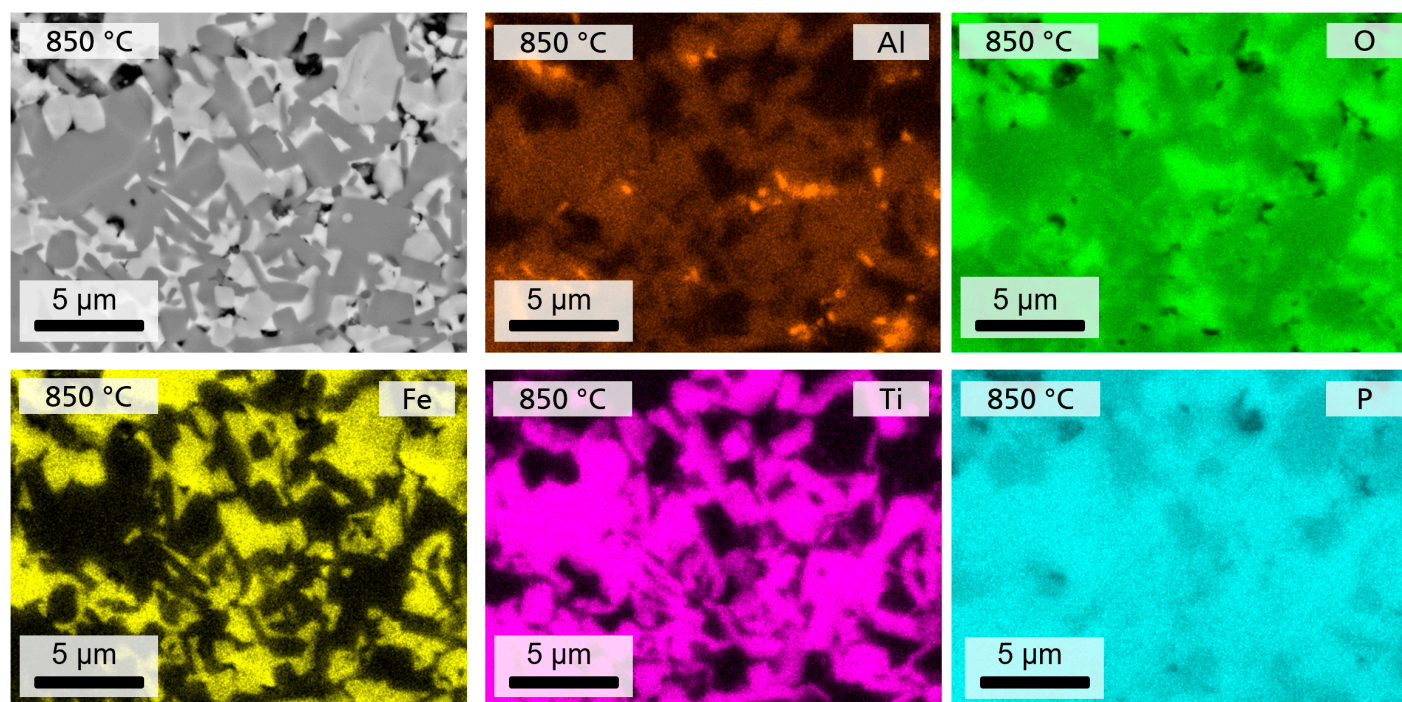


Figure S7. FESEM-EDX mappings of the LATP-LFP microstructure sintered at $T = 850$ °C with partial separation of Al-rich phases and Fe diffusion in Ti-containing phases.

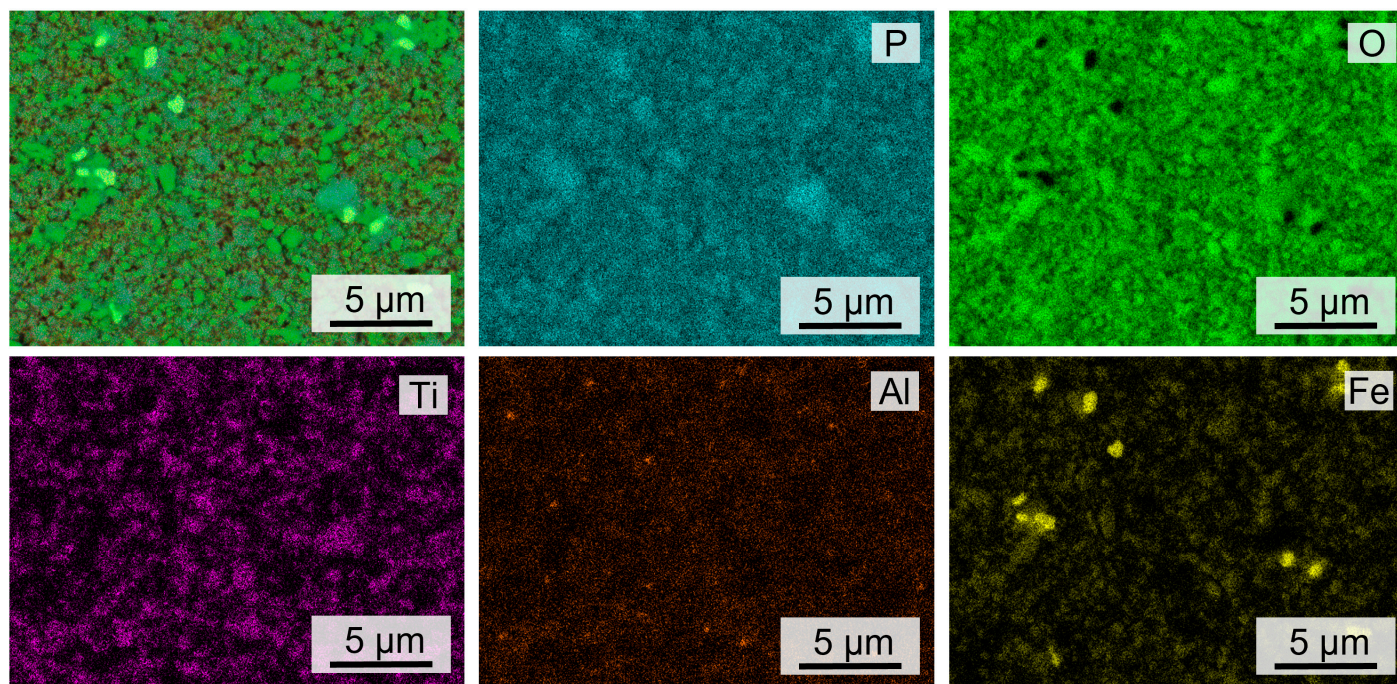


Figure S8. FESEM/EDX mappings of tape-casted LATP-LFP tape after debinding and co-sintering at 850 °C.

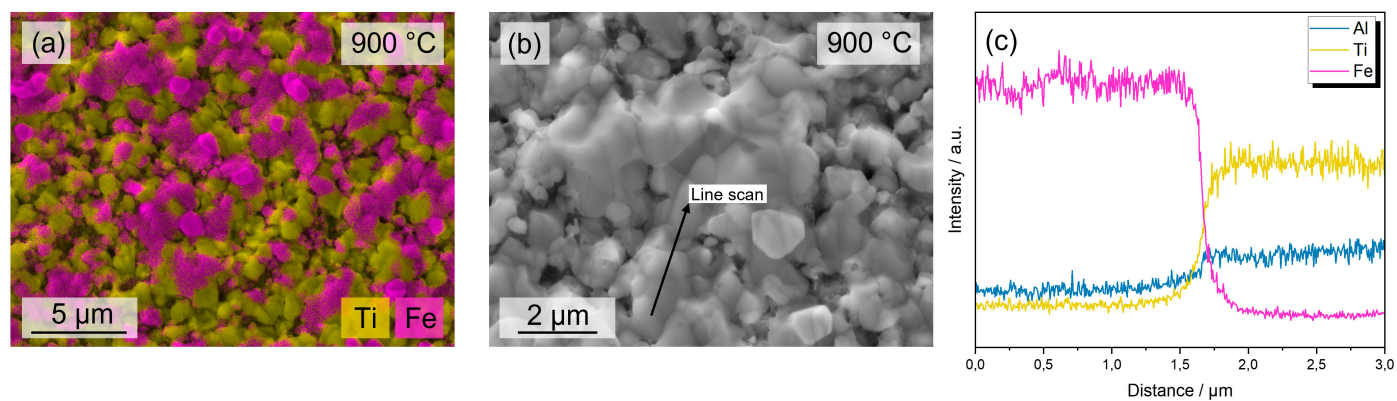


Figure S9. (a) FESEM/EDX mappings of LATP-LFP tape after co-sintering at 900 °C and (b, c) line scan at the grain boundary of the active material and solid electrolyte. The diffusion effects of Fe and Ti at the interfaces are detected.

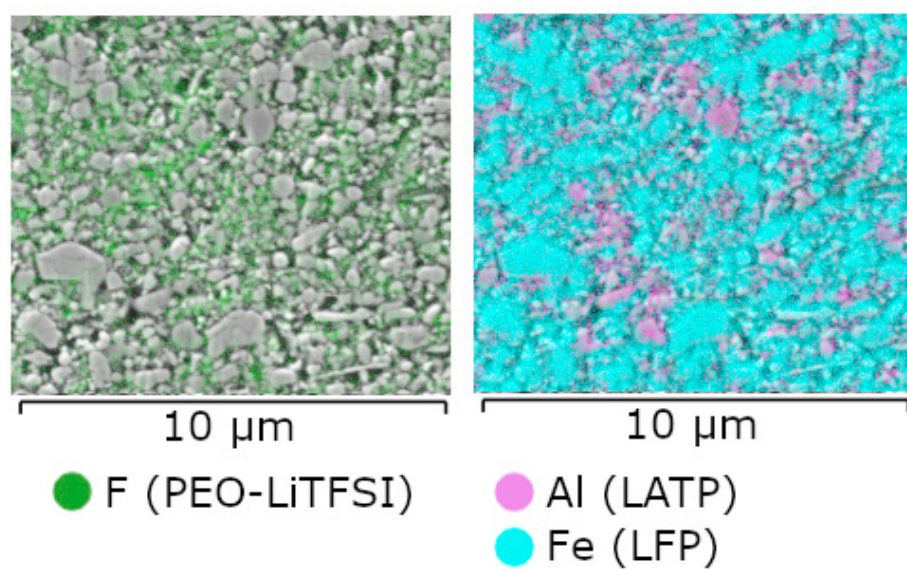


Figure S10. FESEM image and EDX color map showing an even distribution of fluorine (PEO-LiTFSI) between the LATP and LFP particles.